Available online at www.sciencedirect.com
ScienceDirect
Ceramics International 36 (2010) 803–806
CERAMICS INTERNATIONAL
www.elsevier.com/locate/ceramint

Short communication

Preparation and characterization of hydroxyapatite from eggshell

Gréta Gergely [a,*], Ferenc Wéber [a], István Lukács [a], Attila L. Tóth [a], Zsolt E. Horváth [b], Judit Mihály [c], Csaba Balázsi [a]

[a] Ceramics and Nanocomposites Department, Research Institute for Technical Physics and Materials Science, Hungarian Academy of Sciences, Budapest, Hungary
[b] Nanostructures Department, Research Institute for Technical Physics and Materials Science, Hungarian Academy of Sciences, Budapest, Hungary
[c] IR and Raman Spectroscopy Laboratory, Chemical Research Center, Hungarian Academy of Sciences, Budapest, Hungary

Received 20 July 2009; received in revised form 25 August 2009; accepted 7 September 2009
Available online 12 October 2009

Abstract

Hydroxyapatite (HAp) was successfully produced by using recycled eggshell. The observed phases of the synthesised materials were dependent on the mechanochemical activation method (ball milling and attrition milling). The structures of the HAp were characterized by X-ray diffraction, scanning electron microscopy and infrared spectroscopy. Attrition milling proved to be more efficient than ball milling, as resulted nanosize, homogenous HAp even after milling.

Keywords: HAp; Eggshell; Ball milling; Attrition

1. Introduction

Hydroxyapatite (HAp, $Ca_{10}(PO_4)_6(OH)_2$) is among of the few materials that are classified as bioactive, meaning that it will support bone ingrowth and osseointegration when used in orthopaedic, dental and maxillofacial applications [1–3]. Coatings of hydroxyapatite are often applied to metallic implants, especially stainless steels and titanium alloys to improve the surface properties. Hydroxyapatite may be employed in forms such as powders, porous blocks and hybrid composites to fill bone defects or voids. These may arise when large sections of bone have had to be removed or when bone augmentations are required (e.g. dental applications). HAp can be produced from coral [4], seashell [5], eggshell [3,6,7] and also from body fluids [8].

Hydroxyapatite nanopowders have been produced by using eggshell derived raw material and phosphoric acid. The Ca/P mixing ratio 1.67 was determined in an earlier work [9]. The observed phases during the powder synthesis processing were dependent on the mixing ratio (wt.%) of the calcined eggshell and phosphoric acid, the calcination temperature and the duration of the mechanochemical synthesis [10]. HAp structure was characterized by X-ray diffraction (XRD) and scanning electron microsopy (SEM). HAp synthesis by wet chemical methods are known from earlier works [11,12]. The present work aimed to synthesize HAp via mechanochemical activation with the following three objectives: to form HAp from eggshell to compare two mechanochemical activation process: ball milling and attrition milling; and to study the phase stability and powder characteristics.

2. Experimental procedure

Eggshell was collected and their surface was mechanically cleaned. The raw eggshell was calcinated in an air atmosphere at 900 °C. The thermal treatment had two parts: in the first 30 min most of the organic materials were burnt out, whereas in the second part the eggshell transformation into calcium-oxide was obtained (holding time was 3 h). To synthesize calcium phosphate powders, shells were crushed and milled in a ball milling and an attritor milling set up. The ball milling (Fritsch GmBH) is equipped with alumina balls and bowls, the attritor milling (Union Process) was fitted with zirconia tanks and zirconia balls (∅2 mm). The crushed eggshell was reacted by an exothermic reaction with phosphoric acid. The mixtures were milled for 5 h, at 4000 rpm (attritor milling) or for 10 h at

* Corresponding author.
E-mail address: gergelyg@mfa.kfki.hu (G. Gergely).

0272-8842/$36.00
doi:10.1016/j.ceramint.2009.09.020

Table 1
Preparation parameters of hydroxyapatites.

Sample	Raw material	Milling		wt% shell: H_3PO_4	Milling time (h)	Sintering conditions	
		Method	Rpm			Temperature (°C)	Holding time (h)
EA	Eggshell	Attritor milling	4000	50:50	5	–	–
EA _900				50:50	5	900	2
EB	Eggshell	Ball milling	350	50:50	10	–	–
EB_900				50:50	10	900	2

350 rpm (ball milling), for homogenous mixing and to prevent agglomeration of the calcined. The details of the milling procedure, and the samples are presented in Table 1. HAp powders usually degrade at high temperatures, the most common problem being that the CaO phase appears. After milling, a small amount of (approximately 0.5 g) each type of HAp powders were heat treated at 900 °C for 2 h in air atmosphere (Table 1).

The phase composition of the powders was studied by X-ray diffractometry (XRD-Bruker Advance 8D) and Fourier transform infrared spectroscopy (FTIR-Varian Scimitar FTIR spectrometer equipped with broad band MCT detector). The morphological characteristics of the calcined eggshell synthesized powders, were examined by scanning electron microscopy (SEM-LEO 1540 XB).

3. Results and discussion

The morphology of the milled powders is presented in Fig. 1. The samples made by attrition milling are shown in Fig. 1a and b whereas the samples produced by ball milling are shown in Fig. 1c and d. Attrition milling resulted in nanosized grains (Fig. 1a). After the heat treatment at 900 °C, the particle size of 100 nm is characteristic (Fig. 1b). In the case of ball milling, grains sticked together are characterizing the sample (Fig. 1c). Coagulated samples with smooth surfaces are evolving after heat treatment at 900 °C (Sample EB_900, Fig. 1d).

As observed from SEM micrographs, smaller particle size with homogeneous size distribution may be achieved with attritor milling compared to ball milling.

In Fig. 2 X-ray diffractograms of the powder samples are presented. After intensive attrition milling, EA sample (Fig. 2a) contains hydroxyapatite (JCPDS-PDF 74-0565), calcite ($CaCO_3$, JCPDS-PDF 05-0586), monetite (CaHPO4, JCPDS-PDF 071-1760) and hydrogen phosphate (H_3PO_3, JCPDS-PDF072-0518). After heat treatment (900 °C, 2 h) the main phase was hydroxyapatite with some calcite and calcium-oxide (CaO, JCPDS-PDF 037-1497) (Sample EA_900). Powder produced by ball milling (Sample EB) included montetite, hydrogen phosphate and portlandite ($Ca(OH)_2$, JCPDS-PDF

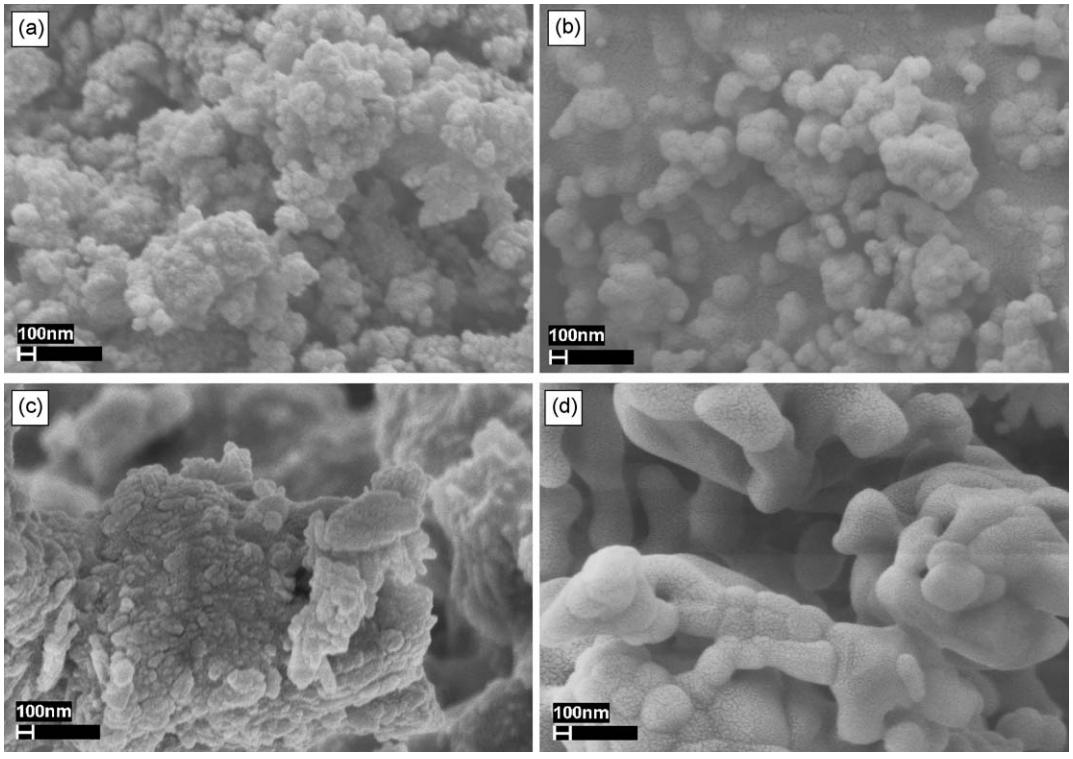

Fig. 1. SEM micrographs of attrition and ball milled samples: (a) EA, (b) EA_900, (c) EB, and (d) EB_900.

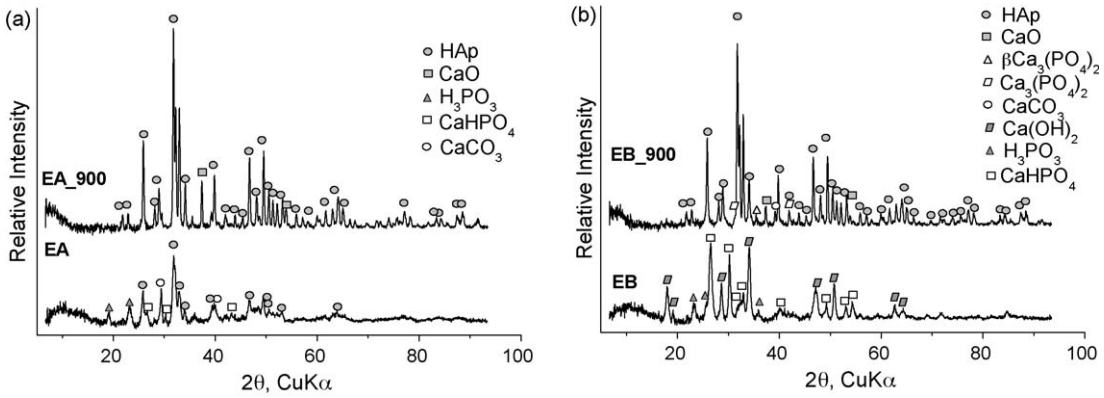

Fig. 2. X-ray diffractograms of the samples: (a) EA and EA_900, (b) EB and EB_900.

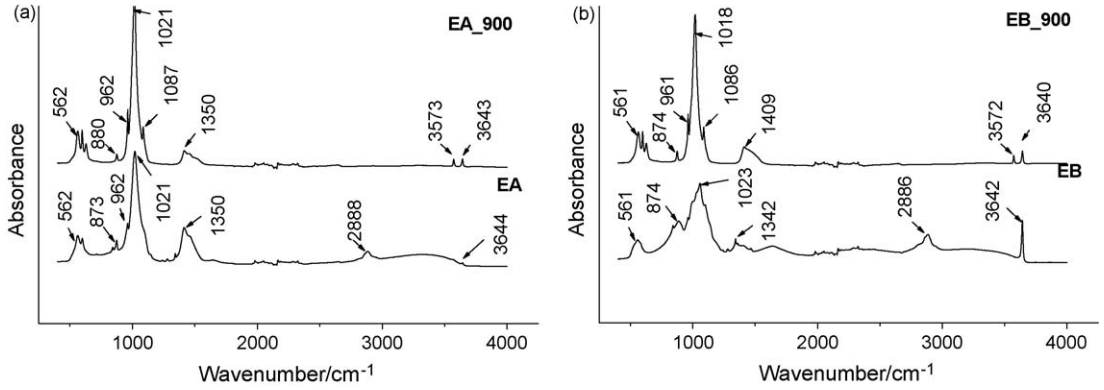

Fig. 3. FTIR spectra of the samples: (a) EA and EA_900, (b) EB and EB_900.

044-1481) (Fig. 2b). Contrary to attrition milled samples the HAp phase was not detected before the heat treatment. Samples were heated at 900 °C for 2 h. After this process hydroxyapatite appeared in Sample EB_900. Some other phases were observed in the Sample EB_900 like: calcite, calcium-oxide, calcium phosphate (β-$Ca_3(PO_4)_2$, JCPDS-PDF 70-2065) and whitlockite ($Ca_3(PO_4)_2$, JCPDS-PDF 002-0786).

The spectrum after attrition milling (EA) (Fig. 3a) resembles the characteristic spectral feature of bone mineral. The spectrum is dominated by the typical PO_4 bands of poorly crystalline apatite phase components of the triply degenerated ν_3PO_4 asymmetric mode at 1021 and 1087 cm^{-1}(shoulder), non-degenerated symmetric stretching mode of ν_1PO_4 at 962 cm^{-1} and components of the triplet of ν_4PO_4 bending mode at 599 and 562 cm^{-1} [13,14]. Carbonate bands are also observed at 1550–1350 cm^{-1} (ν_3), 873 cm^{-1} (ν_2) and 712 cm^{-1} (ν_4). By analogy with bone mineral, the position of carbonate bands (1456, 1415 and 872 cm^{-1}) indicates the formation of a carbonated apatite with B-type substitution (in tetrahedral positions) [15]. The broad band of low intensity in the range 3000–3400 cm^{-1} can be attributed to traces of water incorporated to the structure, together wit the very weak, broad band around 1640 cm^{-1} of H–O–H bending mode. In the OH stretching vibration region, beside the νOH of the hydroxyapatite, surface OH band at 3644 cm^{-1} also appears, probably connected to CaO occurring on the surface. With increasing the temperature, the intensity of surface OH band also increases (EA_900).

FTIR spectrum of EB sample after ball milling shows a complex mixture of different calcium phosphate phases: $CaHPO_4$, $Ca_3(PO_4)_2$ and $Ca_{10}(PO_4)_6(OH)_2$ (Fig. 3b).

This band decreases in matured bone apatite and in highly crystalline hydroxyapatite [13,16]. The pure hydroxyapatite phase with some carbonate substitution is formed only after 900 °C. However, surface OH bands are also present in the spectrum. After heat treatment (EB_900), spectral features of the apatite phase become dominant and above 800–900 °C beside some peaks of carbonate (ν_3 at 1466 and 1409 cm^{-1}, ν_2 at 874 cm^{-1}, ν_4 at 713 cm^{-1}) and surface –OH (νOH at 3640 cm^{-1}) typical bands of well-crystallised hydroxyapatite can be observed (ν_3PO_4 at 1086 and 1018 cm^{-1}, ν_1PO_4 at 961 cm^{-1} and the triplet of ν_4PO_4 at 626, 599 and 561 cm^{-1}) [16,17]. No traces for acid phosphate (HPO_4^{2-} peak around 540–530 cm^{-1}), characteristic for immature bone mineral or incomplete apatite phase can be observed [17].

4. Conclusions

SEM micrographs showed that the ball milling process resulted in micrometer sized coagulated coarse grains with smooth surface, whereas attrition milled samples are characterized by the nanometer size grains. This characteristic morphology being preserved even after firing at high temperature (900 °C). Contrary to ball milling attrition resulted in nanosized and homogeneous HAp even after milling.

Acknowledgement

Thanks to financial support (OTKA 76181).

References

[1] E. Saiz, L. Gremillard, G. Menendez, P. Miranda, K. Gryn, A.P. Tomsia, Preparation of porous hydroxyapatite scaffolds, Materials Science and Engineering C 27 (2007) 546–550.
[2] K. de Groot, Bioceramics consisting of calcium phosphate salts, Biomaterials 1 (1980) 47–53.
[3] E.M. Rivera, M. Araiza, W. Brostow, M. Victor, J.R. Castano, R. DıazEstrada, J. Hernandez, R. Rodrıguez, Synthesis of hydroxyapatite from eggshells, Materials Letters 41 (1999) 128–134.
[4] U. Ripamonti, J. Crooks, L. Khoali, L. Roden, The induction of bone formation by coral-derived calcium carbonate/hydroxyapatite constructs, Biomaterials 30 (2009) 1428–1439.
[5] K.S. Vecchio, X. Zhang, J.B. Massie, M. Wang, C.W. Kim, Conversion of bulk seashells to biocompatible hydroxyapatite for bone implants, Acta Biomaterialia 3 (2007) 910–918.
[6] S.J. Leea, S.H. Oh, Fabrication of calcium phosphate bioceramics by using eggshell and phosphoric acid, Materials Letters 57 (2003) 4570–4574.
[7] C. Balázsi, F. Wéber, Z. Kövér, E. Horváth, C. Németh, Preparation of calcium-phosphate bioceramics from natural resources, Journal of the European Ceramic Society 27 (2007) 1601–1606.
[8] A.C. Tas, Synthesis of biomimetic Ca-hydroxyapatite powders at 373C in synthetic body fluids, Biomaterials 21 (2000) 1429–1438.
[9] C. Balázsi, Z. Kövér, E. Horváth, C. Németh, Z. Kasztovszky, S. Kurunczi, F. Wéber, Examination of calcium-phosphates prepared from eggshell, Materials Science Forum 537/538 (2007) 105–112.
[10] K.C.B. Yeong, J. Wang, S.C. Ng, Mechanochemical synthesis of nanocrystalline hydroxyapatite from CaO and CaHPO, Biomaterials 22 (2001) 271–275.
[11] A. Slosarczyk, E. Stobicrska, Z. Paszkicwicz, M. Gawlicki, Calcium phosphate materials prepared from precipitate with various calcium :phosphororus molar ratios, J. Am. Ceram. Soc. 79 (1996) 2539–2544.
[12] N.O. Engin, A.C. Tas, Preparation of porous $Ca_{10}(PO_4)_6(OH)_2$ and $\beta Ca_3(PO_4)_2$ bioceramics, Journal of American Ceramic Society 83 (2000) 1581–1584.
[13] L.M. Miller, V. Vairavamurthy, M.R. Chance, R. Mendelsohn, E.P. Paschalis, F. Betts, A.L. Boskey, In situ analysis of mineral content and crystallinity in bone using infrared micro-spectroscopy of the $\nu 4$ PO_4^{3-} vibration, Biochimica et Biophysica Acta 1527 (2001) 11–19.
[14] F. Zafarina Zakaria, J. Mihály, I. Sajó, R. Katona, L. Hajba, F. Abdul Aziz, J. Mink, FT-Raman and FTIR spectroscopic characterization of biogenic carbonates from Philippine venus seashell and Porites sp., Coral Journal of Raman Spectroscopy 39 (2008) 1204–1209.
[15] C. Rey, V. Renugopalakrishnan, B. Collins, M.J. Glimcher, Calcified Tissue International 49 (1991) 251–258.
[16] Anna Slosarczyk, Czeslawa Paluszkiewicz, Marek Gawlicki, Zofia Paszkiewicz, The FTIR spectroscopy and QXRD studies of calcium phosphate based materials produced from the powder precursors with different Ca/P ratios, Ceramics International 23 (1997) 297–304.
[17] V.C. Farmer, The Infrared Spectra of Minerals, Bartholomew Press, Dorkung, Surrey, 1974, p. 390.